AN IMPROVED Q-TOMOGRAPHY METHOD FOR ESTIMATION OF SEISMIC ATTENUATION THROUGH NON-LINEAR INVERSION

HONGXU WANG[1], ZIQI JIN[2], DEGUANG TIAN[1] , WEI XU[1] and YUSONG TAN[3]

[1] Research Institute of Exploration and Development of Daqing Oilfield Company Ltd., Kexue Road, Daqing 163712, P.R. China. 254605038@qq.com
[2] China University of Petroleum-Beijing, 18 Fuxue Road, Changping, Beijing 102249, P.R. China. 13945920057@126.com
[3] CNPC Well Logging Company Ltd., Yanshan Road, Renqiu 062552, P.R. China. 414022746@qq.com

(Received March 6, 2016; revised version accepted December 14, 2016)

ABSTRACT

Wang, H., Jin, Z., Deguang, T., Xu, W. and Tan, Y., 2017. An improved Q-tomography method for estimation of seismic attenuation through non-linear inversion. *Journal of Seismic Exploration*, 26: 171-182.

Due to the viscous-elastic properties of subsurface media, seismic waves experience a loss of amplitude and distortion of phase during propagation. Various methods have been designed to compensate for this attenuation (Q-values) to achieve a high seismic resolution. Traveltime attenuation tomography is an efficient method for estimation of the Q-distribution using inversion. The method updates an initial Q-guess to the true Q-distribution. The Q-update amount is associated with the difference between the simulated traveltime attenuation (SAT) response of the model data and the recorded traveltime attenuation (RAT) of field data. The inversion system is a non-linear process that considers the case in which the travel time of the seismic wave depends on the Q-value to be estimated. Therefore, it is reasonable to calculate the Q-value using the non-linear inversion technique. The accuracy of RAT is essential for Q-tomography. Minute errors in the attenuation of the traveltime can cause unreasonable Q-inversion results. A stabilized method is designed to improve the accuracy of RAT by statistically selecting the optimum frequency band for regression and excluding unreasonable results. Synthetic and field data examples demonstrate the feasibility and effectiveness of this method for Q-estimation. Using a more accurate Q-distribution, seismic resolution can be improved after Q-compensation migration.

KEY WORDS: Q-, tomography, attenuation, non-linear inversion, ray tracing.

0963-0651/17/$5.00

INTRODUCTION

The viscous-elastic properties of subsurface media cause a loss of amplitude and distortion of phase in seismic waves. To quantify this attenuation for characterization of rock and fluid properties and to compensate the attenuation for high seismic resolution, it is necessary to estimate the amount of attenuation during propagation. Because the Q-value is the factor used to quantify the attenuation amount, various methods have been designed for Q-estimation. These methods can be grouped into three categories: time-domain Q-estimation, frequency-domain Q-estimation and tomography inversion. Time-domain Q-estimation methods are not recommended because they encounter difficulties in separating intrinsic attenuation from spherical spreading loss and transmission loss, etc. Spectral ratio and centroid frequency shift are two widely used Q-estimation methods in the frequency domain. By picking obvious seismic events at two different travel times, the Q-value between strata can be estimated based separately on the change in reflection amplitude spectrum and the location of the centroid. However, the methods cannot detect variation of Q-values in the vertical and lateral direction in a detailed manner. In addition, frequency-domain Q-estimation methods are affected by noise levels and the choice of frequency band for the data.

Q-tomography inversion has been applied for Q-estimation in seismic processing for decades. According to different methods of traveltime attenuation calculation in field data, these methods can be grouped into two categories: centroid frequency shift Q-tomography and spectral ratio Q-tomography.

Centroid frequency shift Q-tomography reconstructs the Q-distribution using the downshift of the centroid of the signal spectrum as the input (Liao and McMechan, 1997; Quan and Harrist, 1997). Many scientists have reported improved methods. Cao (2010) used the amplitude ratios between neighbouring reflection rays to overcome difficulty in estimating the source radiation patterns. Hu et al. (2011) added a source-amplitude-spectrum fitting function to handle asymmetric source amplitude spectra and an active-set method to force the reconstructed Q-values to fall within their physical bounds. He and Cai (2012) corrected migration stretch and ghost effects of CIG gathers before application of centroid frequency shift tomography. He et al. (2014) proposed an adaptive correction technique to correct for any deviation from the explicit relationship between the attenuation effect and different accumulated travel time attenuation.

Brzostowski and McMechan (1992) used the spectral ratio information to obtain the Q-distribution by solving the linear system using simultaneous iterative reconstruction technology (SIRT) and subsequently applied spectral ratio Q-tomography on 3D surface-survey field data. Rickett (2006) applied the diagonal weighting function and a constraint operator to ensure that model components behave reasonably in Q-tomography for interval Q-estimation. The

improvement showed additional accuracy using noise suppression and Q-value constraints, but the method is still based on a constant Q-value assumption in the horizontal orientation. Considering the influence of frequency variation on Q-estimation, Xin (2009) divided the seismic data into different frequency bands and calculated the corresponding Q-value within each band. Valenciano and Chemingui (2012, 2013) further modified Rickett's method for the variable Q-value in the horizontal direction and solved the linear inversion scheme using conjugate gradient methods with 3D regularization. Xin et al. (2015) measured traveltime attenuation information from both pre-migration data and post-migration data using frequency bands with a good signal-to-noise ratio (SNR).

Noting that all of the methods described above ignore the traveltime attenuation information, we introduce traveltime attenuation tomography for estimation of the Q-distribution. Improvements in the accuracy of RAT calculations are achieved by statistically selecting the optimum frequency band for regression and excluding unreasonable results. We modify the logarithmic spectrum ratio (LSR) method (Sun et al., 2014), which is used in interval Q-calculation, and apply it to shot gathers for RAT calculation using field data. The discrepancy between the RAT and SAT is associated with the Q-update amount. By minimizing the discrepancy, the actual Q-distribution can be captured using non-linear inversion.

METHODOLOGY

Traveltime attenuation tomography through non-linear inversion

In a surface seismic survey, waves travel though the earth and are reflected back to the surface while carrying amplitude and traveltime information. Traveltime information is used in tomography to detect the Q-distribution. For a two-dimensional area, tomography divides the area into cells, each with a constant velocity v and Q-value. A ray is divided by the cells during travel through this area, as shown in Fig. 1.

The traveltime attenuation t_i^* of the ray can be expressed as:

$$t_i^* = \sum_j (l_{ij}/v_{ij})Q_j^{-1} = \sum_j t_{ij}Q_j^{-1} \quad , \tag{1}$$

where l_{ij} is the distance in the j-th cell, and t_{ij} is the traveltime in the j-th cell of the i-th ray.

Eq. (1) can be rewritten in matrix notation:

$$\mathbf{T}Q-= t^* \quad , \tag{2}$$

where the matrix **T** contains elements $t_{i\,j}$ calculated by ray tracing, Q is the Q-value vector, and t^* is the RAT vector which can be calculated by the modified LSR method. The method and its corresponding statistical technology are presented later in this paper.

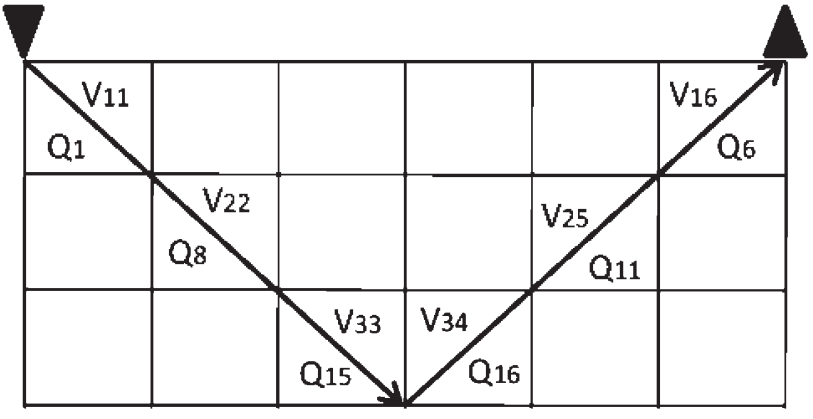

Fig. 1. Ray path in the grid area for tomography. The ray travels from the source, is reflected at the bottom and is received by the receiver at the surface. In each cell, the corresponding velocity and Q-value are constants.

Assuming that the traveltime of the seismic wave is dependent on the Q-values to be estimated, the inversion eq. (2) becomes non-linear. If the seismic response is a non-linear function of the model parameters, the non-linear approach to geophysical inversion iteratively updates the parameters for a given geophysical model (Perez, 2004). Thus the Q-values are calculated iteratively by solving the linear approximation from an initial Q-guess. The initial Q-guess is usually incorrect. The error between the initial Q-guess and the true Q-distribution of the earth δQ_j^{-1} can be expressed as:

$$\delta t_i^* = t_{real}^* - t_{model}^* = \sum t_{i\,j} \delta Q_j^{-1} \quad , \tag{3}$$

where t_{real}^* is the RAT calculated from field data, and t_{model}^* is the SAT calculated in the Q-model via ray tracing. The full matrix form can be expressed as:

$$\begin{bmatrix} t_{11} & \cdots & t_{1n} \\ \vdots & \ddots & \vdots \\ t_{m1} & \cdots & t_{mn} \end{bmatrix} \times \begin{bmatrix} \delta Q_1^{-1} \\ \vdots \\ \delta Q_n^{-1} \end{bmatrix} = \begin{bmatrix} \delta t_1^* \\ \vdots \\ \delta t_m^* \end{bmatrix} \quad . \tag{4}$$

The final Q-result Q_{final} is given by:

$$Q_{final} = Q_{model}/(1 + Q_{model} \cdot \delta Q^{-1}) \quad . \tag{5}$$

The inversion system is solved by LSQR. The accuracy of the results can be improved by increasing the number of iterations. In practice, considering the efficiency of the inversion, the number of iterations should not be excessively large.

RAT CALCULATION WITH STATISTICAL METHOD

The modified LSR method is used to calculate RAT with field data,. We stabilize the process by introducing a statistical method that can reduce the error of RAT. The conventional LSR method is expressed in the following equation (Sun et al., 2014):

$$\ln[B(t_2,f)/B(t_1,f)] = \ln(G) - \pi f(t_2 - t_1)/Q- \quad , \tag{6}$$

where f is the frequency, $B(t_1,f)$ and $B(t_2,f)$ are the seismic wave instantaneous amplitude spectra at travel time t_1 and t_2, respectively, and G is a frequency-independent factor. The effective Q-value in a layer between travel time t_1 and t_2 is estimated using linear regression. We modify eq. (6) and use it for RAT calculation from the shot gathers:

$$\ln[R(t,f)/S(t_0,f)] = \ln(G) - \pi f \sum (t_{i\,j}/Q_{i\,j}) = a + bt^* \quad , \tag{7}$$

where $t^* = t_{i\,j}/Q_{i\,j}$ denotes the attenuation travel time, $t_{i\,j}$ and $Q_{i\,j}$ denote the traveltime and Q-value in the cell (i,j) along the travel path, $S(t_0,f)$ is the amplitude spectrum of the source wave, and R(t,f) is the amplitude spectrum of the wave at a certain time t, and a denotes the frequency-independent attenuation term. The estimation of slope in the spectral ratio b is influenced by the frequency-independent factor G. We calculate the G factor first by picking the intercept term from the linear regression and removing it prior to RAT calculation. As a result, RAT can be expressed by:

$$t^* = \ln\{[R(t,f)/a]/S(t_0,f)\}/(-\pi f) \quad . \tag{8}$$

A traveltime attenuation constraint can be set as the frequency-independent factor associated with an intrinsic loss of less than one:

$$G \leq 1 \quad . \tag{9}$$

By substituting expression (9) into eq. (8), and we can force the

attenuation traveltime to fall within the physical bounds:

$$t^* \leq \{\ln[R(t,f)/S(t_0,f)] - \ln(1)\}/(-\pi f) \quad . \tag{10}$$

The choice of frequency band has great effects on the result of the RAT calculation, as in the case of the LSR method. Assuming the attenuation is obvious at the dominant frequency and its neighbouring frequencies, an optimum frequency band is statistically selected for regression. We calculate a set of RAT from different frequency bands centred at the dominant frequency f_{dom},

$$\begin{aligned} t^*_{f_1}, f_1 &\in (f_{dom}-1, f_{dom}+1) \\ t^*_{f_2}, f_2 &\in (f_{dom}-2, f_{dom}+2) \\ &\vdots \\ t^*_{f_n}, f_n &\in (0, 2 * f_{dom}) \end{aligned} \quad . \tag{11}$$

The final result can be picked from the median of the RAT sequence:

$$t^* = \text{median}(t^*_{f_1}, t^*_{f_2}, \cdots, t^*_{f_n}) \quad . \tag{12}$$

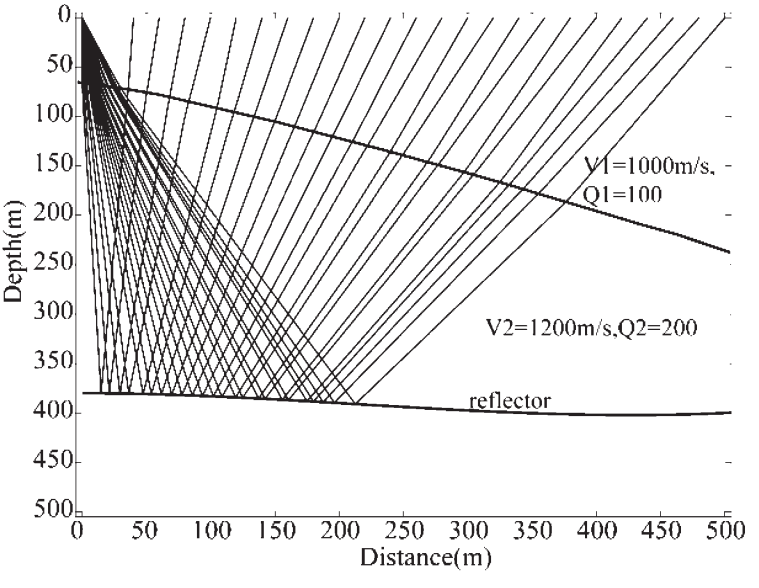

Fig. 2. Salt dome model with ray paths of the first shot. Rays refract while travelling through the dipping interface from 60 m depth to 200 m depth and reflect at the reflector near 400 m depth. The background velocity is 1000 m/s with a Q-value of 100. The salt has a velocity of 1200 m/s with a Q-value of 200.

MODEL TEST FOR THE PROPOSED Q-TOMOGRAPHY AND EFFECTIVENESS ANALYSIS

The salt dome model presented below (Fig. 2) is used to demonstrate the proposed method and to analyse the effect of the traveltime attenuation discrepancy on the inversion results of the Q-distribution. The model is constructed using 50 × 50 square cells and is 50 cells wide (500 m) and 50 cells deep (500 m). The receivers and shots are evenly distributed at the surface.

TRAVELTIME ATTENUATION CALCULATION

Ray tracing is applied to trace the rays from the sources to the receivers. The rays of the first shot are depicted in Fig. 2. Synthetic data are obtained using viscous-elastic finite-difference scheme forward modelling. Seismic events reflected from the reflector are windowed for traveltime attenuation calculation. Because the choice of frequency band is critical to the modified LSR method and the result of RAT, the stabilized technique introduced above and the conventional method are both applied to illustrate improvement in the accuracy

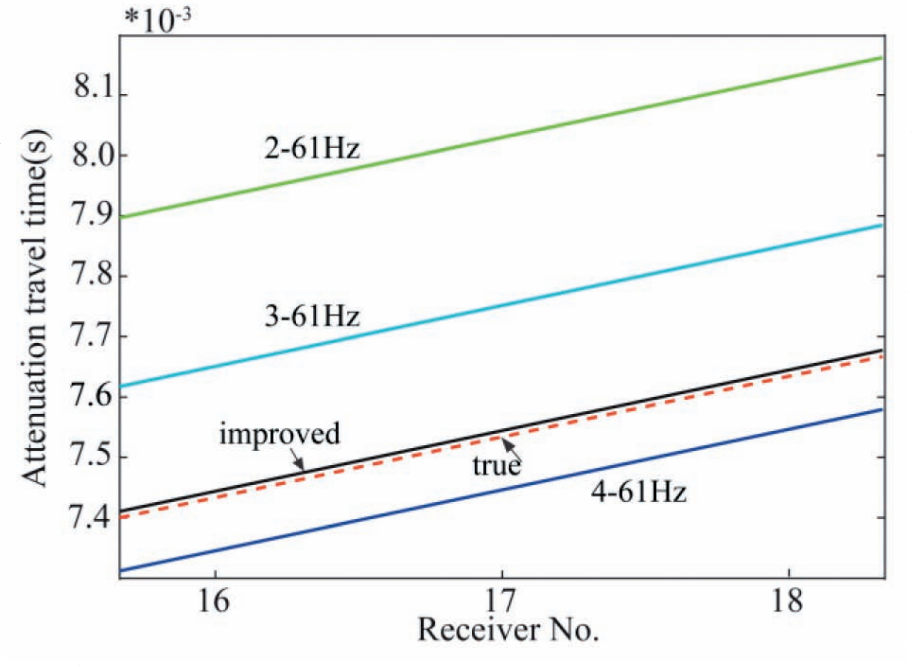

Fig. 3. Comparison of traveltime attenuations between the 16th and 18th receivers using the improved and conventional methods. The accurate result of the improved method (solid black line) agrees well with the true value (dotted line). The results of conventional method are not stable as the frequency band slightly changes.

of the result. Different frequency bands (2-61 Hz, 3-61 Hz, and 4-61 Hz) are chosen for the conventional method. These frequency bands are nearly the same except for a small perturbation at the low frequency end. The results from the conventional and the improved methods are shown in Fig. 3. Statistically optimum frequency band selection plus the RAT constraint produce a more accurate result. Although the conventional method gives unreasonable results due to poor selection of the frequency band, the error grows even larger as the frequency band slightly changes towards the low frequency end (the blue curve of frequency 2-61 Hz). The selected frequency band can be corrected (towards 4-61 Hz) after several iterations by applying certain types of criteria in the conventional method, but it is a time-consuming and complicated process compared with the improved technique that can solve the problem in one step.

Two types of RAT calculations are used as seismic responses in the following inversion process to illustrate the effect of RAT error on the inversion result.

ERROR ANALYSIS OF TRAVELTIME ATTENUATION ON INVERSION RESULTS

The Q-distribution can be derived by solving eq. (4) and (5) using the two types of traveltime attenuation calculated above as input. The inversion results are shown in Fig. 4, where (c), (d) and (e) in this figure are the inversion results produced using different traveltime attenuation as inputs calculated within different frequency bands (4-61 Hz, 3-61 Hz, and 2-61 Hz). The interfaces of these Q-distribution are difficult to discern, especially for the 2-61 Hz frequency band. The errors in these Q-values are approximately 6, 13 and 20 percent of the true value, respectively. The result (b) of the proposed tomography is notably close to the true value and the interface is much easier to detect, both the horizontal and vertical variations of Q-values can be detected quite well. The error of the proposed method is less than 0.1 percent of the true value.

The results from the conventional method display large errors even though the traveltime attenuation appears to agree well with the true value. Minute errors in traveltime attenuation cause large errors in the estimated Q-result. Therefore, it is necessary to account for the traveltime attenuation error and to improve the accuracy of traveltime attenuation. Q-values estimated by the proposed method are notably close to the true value.

FIELD DATA APPLICATIONS

The proposed method is also applied to field data. We calculate the Q-distribution at depths above of 8000 m using Q-tomography. Seismic events

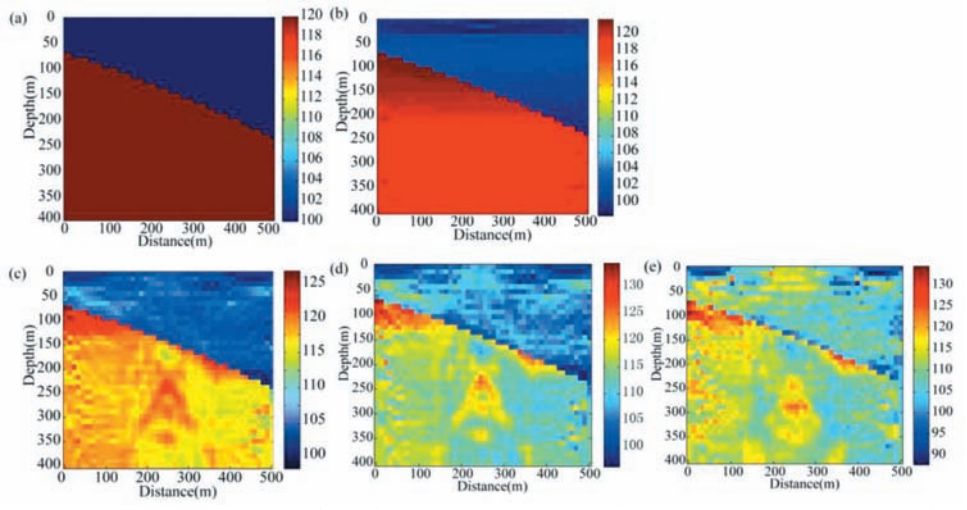

Fig. 4. Comparison of the inversion results of the Q-distribution using different traveltime attenuations as input. (a) Initial Q-distribution. (b) Q-distribution calculated by the proposed method. (c) Q-distribution calculated by the conventional method using the 4-61 Hz frequency band information. (d) Q-distribution calculated by the conventional method using the 3-61 Hz frequency band information. (e) Q-distribution calculated by the conventional method using the 2-61 Hz frequency band information.

of shot gathers at a traveltime of 4.0 s are windowed for RAT calculation. The initial Q-guess is set to a constant value of 100. The final Q-distribution is shown in Fig. 5 as calculated by the proposed method.

Q-compensation migration is applied for attenuation compensation using the Q-values in Fig. 5. Fig. 6(a) shows the original common reflection point (CRP) gather after migration without any attenuation compensation. The CRP gather in Fig. 6(b) shows improvements in the events with Q-values from the conventional method. The proposed method further improves the amplitude and phase of the events in Fig. 6(c), especially the events at 2.9 s and 3.1 s (arrows).

In this section, we take the AVO curve of the synthetic CRP gathers from the well data as the quantitative criteria. The AVO curve calculated from the proposed method is closer to the criteria with the same trend, whereas the AVO curves calculated from the conventional method experience larger errors, especially for the middle offset portion. The accuracy of the amplitude and phase compensation can be quantitatively tested using the AVO properties in the CRP gathers (Fig. 7). The stack profile of the CRP gathers produce higher resolution and a wider frequency band (Fig. 8). The Q-values estimated by the

proposed method are more accurate, and the compensation for amplitude and phase reveals more credible geological information for further reservoir prediction.

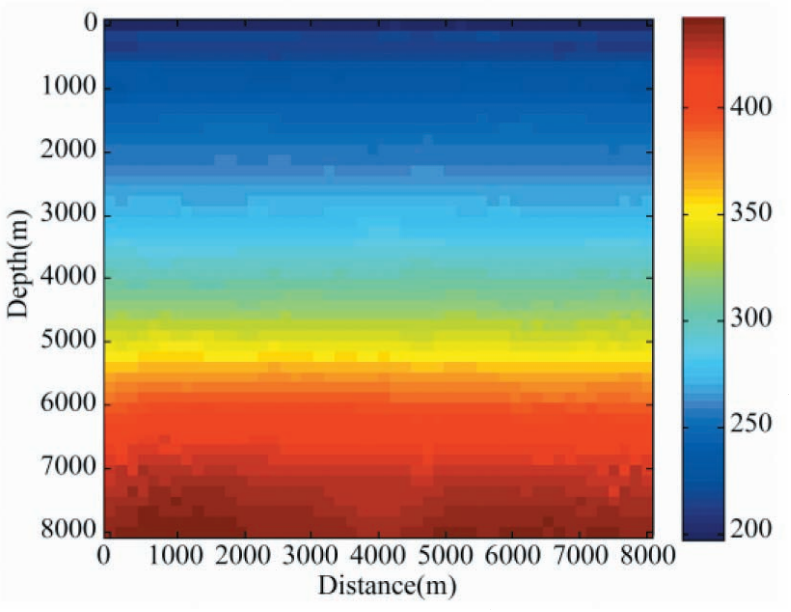

Fig. 5. Inversion results of the Q-distribution using the proposed method. The area is constructed of 80 x 80 square cells and is 80 cells wide (8000 m) and 80 cells deep (8000 m).

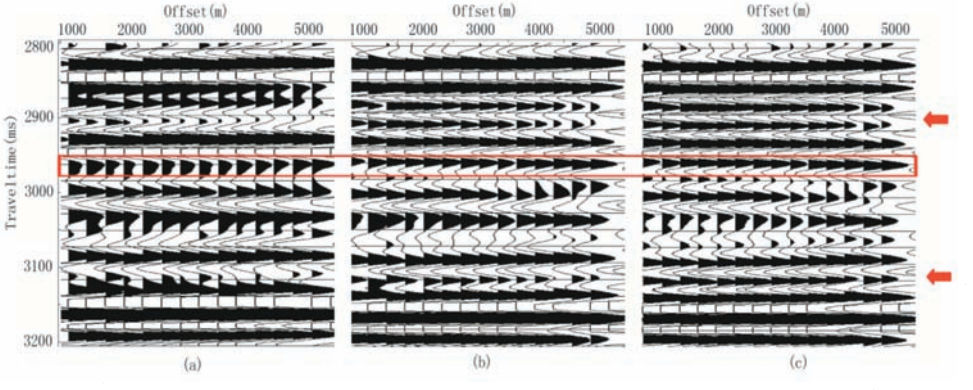

Fig. 6. Comparison of migration gathers. (a) Migration gather without attenuation compensation. (b) Migration gather with attenuation compensation using the Q-values of the conventional method. (c) Migration gather with attenuation compensation using the Q-values of the proposed method. The arrows point to the events with obvious improvements in amplitude and phase using more accurate Q-values. The events in the rectangle are used in AVO analysis.

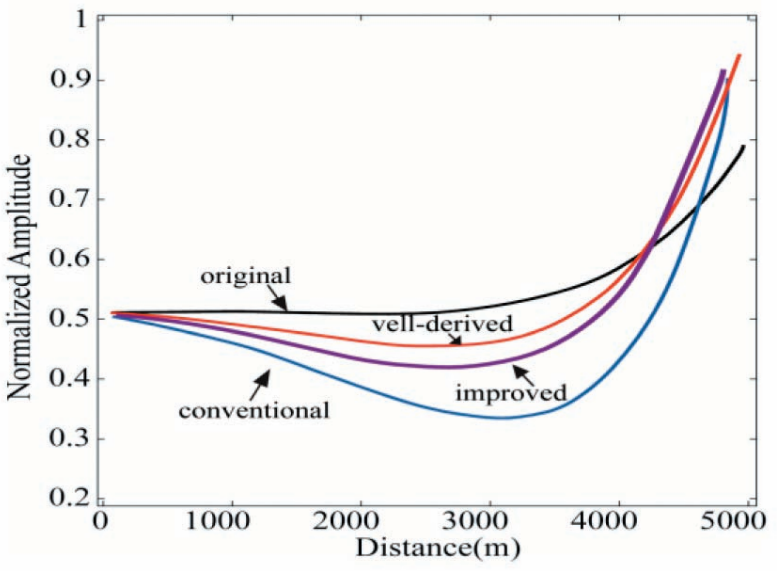

Fig. 7. Comparison of AVO curves after migration using the events in the rectangle in Fig. 8. The amplitudes are normalized, and four curves are set to the same starting point for comparison.

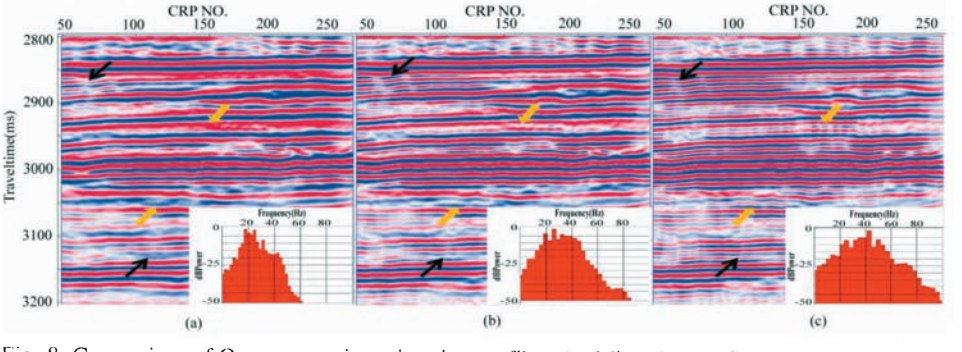

Fig. 8. Comparison of Q-compensation migration profiles. (a) Migration profile without attenuation compensation. (b) Migration profile with attenuation compensation using the Q-values of the conventional method. (c) Migration profile with attenuation compensation using the Q-values of the proposed method. The arrows point to the events with obvious improvements.

CONCLUSIONS

In this work, we calculate the Q-distribution using traveltime attenuation Q-tomography via non-linear inversion on both synthetic and field data. Q-value variation in both the horizontal and vertical direction can be clearly detected for further attenuation compensation and reservoir prediction. Seismic resolution is improved with more accurate Q-distribution applied in the Q-compensation migration.

The key factor that affects the efficiency of the proposed method is the traveltime attenuation calculation. The accuracy of traveltime attenuation is essential for Q-tomography. For RAT calculation, a small perturbation of the frequency band always leads to error in the traveltime attenuation. The proposed method avoids the instability problem by statistically selecting the optimum frequency band for regression.

In the RAT calculation, only the effect of the frequency band on the result of RAT is discussed. Other factors in the field data might also cause errors in traveltime attenuation, such as noise and the thin layer effect, and should be considered. To exclude unreasonable Q-values, we found that the frequency-independent factor can be used as a traveltime attenuation constraint. For further study, many other different constraints, such as well data, can be included to decrease the size of the solution space.

REFERENCES

Brzostowski, M.A. and McMechan, G.A., 1992. 3-D tomographic imaging of near-surface seismic velocity and attenuation. Geophysics, 57: 396-403.

Cao, H., 2010. Reflection attenuation tomography: a field example. Expanded Abstr., 80th Ann. Internat. SEG Mtg., Denver: 2815-2819.

He, Y. and Cai, J., 2012. Q-tomography towards true amplitude image and improve sub-karst image. Expanded Abstr., 82nd Ann. Internat. SEG Mtg., Las Vegas: 1-5.

He, Y., Xin, K. and Xie, Y., 2014. Tomographic inversion for background Q-estimation using adaptively corrected centroid frequency shift. Expanded Abstr., Internat. Geophys. Conf., Beijing: 651-655.

Hu, W., Liu, J., Bear, L. and Marcinkovich, C., 2011. A robust and accurate seismic attenuation tomography algorithm. Expanded Abstr., 81st Ann. Internat. SEG Mtg., San Antonio: 2727-2731.

Liao, Q. and McMechan, G.A., 1997. Tomographic imaging of velocity and Q, with application to crosswell seismic data from the Gypsy Pilot Site, Oklahoma. Geophysics, 62: 1804-1811.

Perez, M., 2004. Traveltime Tomography in Isotropic and Transversely Isotropic Media. Ph.D. thesis, Univ. of Alberta, Calgary.

Quan, Y. and Harrist, J.M., 1997. Seismic attenuation tomography using the frequency shift method. Geophysics, 62: 895-905.

Rickett, J., 2006. Integrated estimation of interval-attenuation distributions. Geophysics, 71: A19-A23.

Sun, S.Z., Wang, Y., Sun, X. and Li, C., 2014. Estimation of Q-factor based on pre-stack CMP gathers and its application to compensate attenuation effects. Expanded Abstr., 84th Ann. Internat. SEG Mtg., Denver: 3709-3714.

Valenciano, A.A. and Chemingui, N., 2012. Viscoacoustic imaging: tomographic Q-estimation and migration compensation. Expanded Abstr., 82nd Ann. Internat. SEG Mtg., Las Vegas: 1-5.

Valenciano, A.A. and Chemingui, N., 2013. Tomography and migration in viscoacoustic media. Expanded Abstr., 13th Internat. Congr. Brazil. Geophys. Soc., Rio de Janeiro: 1299-1303.

Xin, K., 2009. 3-D tomographic Q-inversion for compensating frequency dependent attenuation and dispersion. Expanded Abstr., 79th Ann. Internat. SEG Mtg., Houston: 4014-4018.

Xin, K., Xie, Y. and He, Y., 2015. Robust seismic reflection Q-tomography through adaptive measurement of spectral features. Expanded Abstr., 24th Internat. Geophys. Conf., Perth: 1-4.